

Hysteresis, neural avalanches, and critical behavior near a first-order transition of a spiking neural network

Silvia Scarpetta,^{1,2} Ilenia Apicella,³ Ludovico Minati,⁴ and Antonio de Candia^{2,5}

¹*Dipartimento di Fisica “E. Caianiello,” Università di Salerno, Fisciano (SA), Italy*

²*INFN, Sezione di Napoli, Gruppo Collegato di Salerno, Italy*

³*Dipartimento di Fisica e Astronomia “G. Galilei,” Università di Padova, Italy*

⁴*Complex Systems Theory Department, Institute of Nuclear Physics Polish Academy of Sciences (IFJ-PAN), Kraków, Poland*

⁵*Dipartimento di Fisica “E. Pancini,” Università di Napoli Federico II, Complesso Universitario di Monte Sant’Angelo, via Cintia, 80126 Napoli, Italy*



(Received 4 December 2017; revised manuscript received 9 March 2018; published 7 June 2018)

Many experimental results, both *in vivo* and *in vitro*, support the idea that the brain cortex operates near a critical point and at the same time works as a reservoir of precise spatiotemporal patterns. However, the mechanism at the basis of these observations is still not clear. In this paper we introduce a model which combines both these features, showing that scale-free avalanches are the signature of a system posed near the spinodal line of a first-order transition, with many spatiotemporal patterns stored as dynamical metastable attractors. Specifically, we studied a network of leaky integrate-and-fire neurons whose connections are the result of the learning of multiple spatiotemporal dynamical patterns, each with a randomly chosen ordering of the neurons. We found that the network shows a first-order transition between a low-spiking-rate disordered state (down), and a high-rate state characterized by the emergence of collective activity and the replay of one of the stored patterns (up). The transition is characterized by hysteresis, or alternation of up and down states, depending on the lifetime of the metastable states. In both cases, critical features and neural avalanches are observed. Notably, critical phenomena occur at the edge of a discontinuous phase transition, as recently observed in a network of glow lamps.

DOI: [10.1103/PhysRevE.97.062305](https://doi.org/10.1103/PhysRevE.97.062305)

I. INTRODUCTION

Recently, many experimental results have supported the idea that the brain operates near a critical point [1–8], as reflected by power-law distributions of avalanche sizes and durations. The maximization of fluctuations near a critical point is believed to play an important role in the ability of the brain to respond to a wide range of inputs, to process the information in an optimal way [9–13], and to enhance stimulus discriminability [14]. The theoretical framework commonly used to explain this behavior is the branching process, which undergoes a second-order transition when the branching parameter becomes greater than 1. The order parameter, that is, the probability to observe an infinite avalanche, indeed continuously grows above the transition.

On the other hand, metastability and hysteresis are ubiquitous in the brain. They are related to the ability of the brain to sustain stimulus-selective persistent activity for working memory [15]. The brain rapidly switches from one state to another in response to a stimulus, and it may remain in the same state for a long time after the end of the stimulus, suggesting the existence of a repertoire of metastable states. The presence of metastability and criticality could be reconciled if the system is posed near the edge of instability (spinodal line) of a first-order transition.

Recently it has been shown that a simple network of glow lamps (nonlinear devices that share some similarity with leaky neurons) show a critical behavior near the edge of a first-order (discontinuous) phase transition [16].

Critical phenomena and avalanches indeed emerge, not only in second-order transitions, but also in discontinuous ones, as one enters the metastability region and approaches the spinodal curve [17,18]. Close to the spinodal, which for long range interactions denotes the limit of existence of the metastability region, transition precursors are observed which follow power-law scaling having a cutoff diverging to infinity on the spinodal itself; examples are found, for instance, in geophysical phenomena, breakdown of solids, and spontaneous network recovery [19–22]. Bistability with critical features is observed also in nonequilibrium phase transitions [23].

In the present paper, our goal is to understand if a first-order transition with spinodal instabilities may be a correct scenario in neural cortical experiments. We study a simple stochastic leaky spiking model, whose quenched disordered connectivity is the result of learning multiple spatiotemporal patterns, and simulate the spontaneous activity of the network applying a Poissonian noise to individual neurons, related to the spontaneous neurotransmitter release at individual synapses, as well as other sources of inhomogeneity and randomness that determine an irregular background synaptic noise.

We observe that there is a parameter region characterized by a first-order transition which notably shows hysteresis and metastability. The phase transition is between a low activity state, with uncorrelated firing and low rate, and a state characterized by collective activity with high firing rate and high spatiotemporal order, where one of the stored patterns emerges. At higher values of the noise, or smaller network sizes, lifetimes of the states become smaller than the observation

time, so that instead of hysteresis we observe an alternation of the two phases.

Scale-invariant spatiotemporal avalanches occur at the edge of the transition, both inside the hysteresis region (lifetimes of the metastable states longer than the observation time) and near the alternating region (lifetimes smaller than the observation time). Notably, we find that the average avalanche size as a function of the avalanche duration $s(T)$ collapses on a universal power law with an exponent close to the experimental one [24,25].

Another important characteristic of avalanches in the brain is that they contain highly repeatable patterns, both *in vitro* [26] and *in vivo* [27], supporting the hypothesis that scale-free neural avalanches are the signature of a critical behavior in a system that has stored multiple dynamical spatiotemporal patterns. Notably, it has been shown [27] that spike avalanches, recorded from freely behaving rats, form repertoires that emerge in waking, recur during sleep, are diversified by novelty and contribute to object representation. They constitute distinct families of recursive spatiotemporal patterns, and a significant number of those patterns were specific to a behavioral state.

Storing precise spatiotemporal patterns as dynamical attractors of the network is a useful strategy for brain functioning, coding and memory, and many experimental results on the replay of precise spatiotemporal patterns of spikes suggest this possibility [28–33].

Our model captures such additional features of neuronal avalanches, such as the underlying first-order transition between attractor dynamics and quiescence, the stable recurrence of particular spatiotemporal patterns, and the conditions under which these precise and diverse patterns can be retrieved.

Critical avalanches were observed in a leaky integrate-and-fire model of neurons [34,35], but for a single value of the noise and of the size of the system, where no hysteresis was observed, and the type of underlying phase transition was not thoroughly investigated. The role of first-order phase transition for criticality in cortical networks was first pointed out by Ref. [36] and successively elaborated in a leaky integrate-and-fire model [37]. However, as shown in [38], in such models criticality emerges only with a definition of avalanches that takes into account the causality of different firings. Our model exhibits neural avalanches at the edge of a first-order transition, that are identified with the same temporal proximity criterion used in experiments.

II. RESULTS

We study a model of leaky integrate-and-fire neurons, whose connectivity is the result of the learning of multiple spatiotemporal patterns, using a learning rule inspired by spike-time-dependent plasticity (STDP). The emerging spontaneous dynamics is simulated in the presence of noise, with fixed sparse connections, and a small fraction of leader neurons (see Appendix). Two parameters characterize the dynamics. The first is the parameter H_0 that sets the average strength of the connections; the second is the parameter α that is the coupling of each neuron to the noise. The number of neurons goes from $N = 3000$ to $N = 12\,000$, with a number of encoded patterns from $P = 2$ to $P = 10$.

We simulate the spontaneous dynamics of the model in absence of external stimuli as a function of the parameters H_0 and α . Depending on the value of the parameters, two different dynamical states are distinguishable: a quiescence state (“down” state), characterized by uncorrelated spiking with low firing rate, and an active state (“up” state), characterized by a high rate and high spatiotemporal order, and by a long-lasting collective replay of stored patterns.

To characterize the dynamics, we define the instantaneous rate r and the normalized variance F (also called the Fano factor or index of dispersion) as follows:

$$r = \frac{N_{\text{tot}}}{N\Delta}, \quad (1a)$$

$$F = N\Delta \frac{\langle r^2 \rangle - \langle r \rangle^2}{\langle r \rangle}, \quad (1b)$$

where N_{tot} is the total number of spikes over all the network in the time interval Δ , N is the number of neurons of the network, and the average $\langle \dots \rangle$ is evaluated over a sliding window $[t - T, t + T]$. We use a time interval $\Delta = 1$ ms to compute the firing rate and a half-width of $T = 100$ ms for the sliding window. The normalized variance (1b) can also be written as

$$F = \frac{\langle N_{\text{tot}}^2 \rangle - \langle N_{\text{tot}} \rangle^2}{\langle N_{\text{tot}} \rangle}, \quad (2)$$

showing that, if neurons are uncorrelated and Poissonian, then $F = 1$. If $F > 1$ the spiking activity is overdispersed; this corresponds to the existence of clustered activity, with some intervals having a much higher activity than the mean and others a very low activity compared to a Poisson distribution. If on the other hand $F < 1$, activity is underdispersed, with many intervals having spike counts close to the mean.

In Fig. 1, we show the dynamics of the network at fixed noise $\alpha = 0.033$, while we increase the parameter H_0 from 0.1 to 0.3 in 50 s. [Note that throughout the paper the time is always measured as the “physical” time appearing in Eq. (A1), not the CPU time needed to simulate the system.] At low values of H_0 , the spiking rate is low, less than 1 Hz, and normalized variance is near to 1, signaling uncorrelated Poissonian activity (down state). At time $t = 36$ s, when H_0 reaches the value $H_0 = 0.244$, we observe an abrupt transition to a state corresponding to the sustained collective replay of one of the stored patterns with high firing rate (up state). In Figs. 1(a) and 1(b) we show the raster plots of the dynamics in the same interval of time, with neurons ordered on the vertical axis by the two patterns encoded in the network. It can be seen that the transition to the up state corresponds to the replay of one of the stored patterns.

Note that Figs. 1(a) and 1(b) refer to the same spike train. The different ordering on the vertical axis makes the spikes appear in a sawtooth shape when the pattern corresponding to the order is replayed, while they appear as completely random (and deceitfully denser) when another pattern (not corresponding to the ordering of the vertical axis) is replayed. In Fig. 1(c) we show the rate corresponding to the dynamics shown in both raster plots 1(a) and 1(b). It can be seen that, at time $t = 36$ s, when the collective replay of the first patterns starts, the rate sharply increases from a very low value to an average value of 13 Hz, fluctuating between 5 and

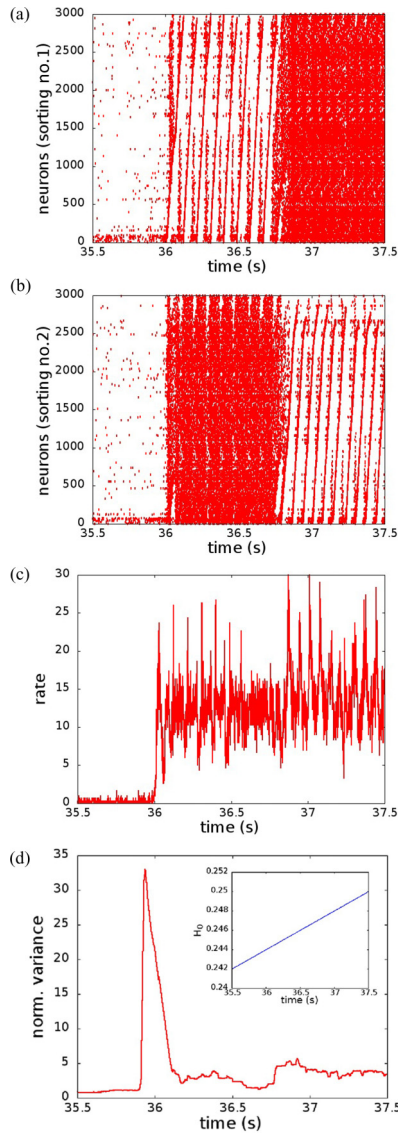


FIG. 1. Spontaneous dynamics for $N = 3000$ at noise $\alpha = 0.033$, showing a transition while we increase parameter H_0 from 0.1 to 0.3 in 50 s. A transition between a quiescence state (down) and a state with emerging of collective replay of stored patterns (up) is shown to occur at time $t = 36$ s, corresponding to a value $H_0 = 0.244$. Raster plots (a) and (b) show the same spontaneous spiking activity with two different sortings of neurons on the vertical axis. In (a) neurons are sorted by the spiking time in pattern 1, while in (b) they are sorted by the spiking time in pattern 2. The replay of the pattern corresponding to the sorting on the vertical axis is apparent by the sawtooth ordering of the spikes: from time $t = 36$ s to time 36.75 s stored pattern number 2 is replayed, while from $t = 36.75$ s stored pattern number 1 is replayed. Note that when a pattern is replayed, there seems to be a lower density of dots due to the fact that the dots overlap. In (c) we show the average instantaneous firing rate, corresponding to both raster plots (a) and (b). The rate is measured as the total number of spikes in a time interval of $\Delta = 1$ ms divided by $N\Delta$. In (d) we show the normalized variance of the firing rate (see text). In the down state normalized variance is equal to 1, while in the up state it goes to values $\sigma > 3$, signaling a non-Poissonian dynamics, with temporal clustering. When the system has a transition to the up state, the firing rate abruptly increases and normalized variance has a peak. Inset: Value of H_0 as a function of time.

30 Hz. Correspondingly, normalized variance F jumps from 1 (Poissonian dynamics) to a value between 2 and 5 (temporally clustered). Note that values of normalized variance greater than 1 are found experimentally in persistent activity in cortical circuits [39]. Exactly at the transition, the normalized variance has a high peak.

A. Hysteresis and first-order transition

The observed discontinuous behavior of the rate and variance suggests that the transition is of a first-order kind. An important characteristic of first-order transitions is hysteresis, so here we investigate if our model actually shows hysteresis while varying parameters H_0 and α . At a fixed value of α , we start with the system in the down state and $H_0 = 0.1$, and cycle H_0 from 0.1 to 0.4 in the first 50 s, and back from 0.4 to 0.1 in the last 50 s. In Fig. 2 we show the instantaneous rate and variance as a function of H_0 in the first half of the run (increasing H_0 , red lines) and in the second half (decreasing H_0 , blue lines). Both rate and variance are averaged over four different runs, with different realizations of stochastic noise.

For low values of the noise, we observe a strong hysteretic behavior of the dynamics. Looking, for example, at Fig. 2(a), where $\alpha = 0.015$, we observe that when H_0 is increased, *down* \rightarrow *up* transitions take place between $H_0 = 0.31$ and 0.32 . As the rate and variance are averaged over four runs, there are actually four different transitions at slightly different values of H_0 , depending on the realization of the stochastic noise.

On the other hand, when H_0 is decreased, *up* \rightarrow *down* transitions take place at lower values of H_0 , in this case around $H_0 = 0.2$. In Figs. 2(b), 2(c) and 2(d), we show the same experiment for higher values of the noise parameter α . When $\alpha \geq 0.45$, the value of the rate and variance does not depend anymore on the history and is equal within fluctuations when H_0 is increased or decreased. Moreover, one can observe multiple back-and-forth transitions *up* \rightarrow *down* and *down* \rightarrow *up*, during the same run, giving rise to a large peak in the variance. In Fig. 3 we show the behavior of the system for a higher value of the number of neurons and number of patterns.

Hysteresis is a hallmark of first-order transitions, characterized by the presence of two (or more) possible states of the system, separated by barriers difficult to overcome. If the system stays in one state, it will tend to remain in that state also when external parameters would favor another one. Therefore the state of the system depends on the past history, for example, if H_0 is being increased or decreased. The nucleation time, i.e., the lifetime of metastable states, depends critically on the range of the connections. If the model is characterized by long range connections, one could expect a “mean-field-like” behavior, with the transitions from the metastable to stable states happening on the spinodal lines. However, in our case, albeit the connections do not depend on distance (that is, they are long range), the number of units is not very large, so we expect that at any point in the space of parameters there will be a nucleation time sufficient to switch the system from one state to the other that can also be interpreted as a typical lifetime of the state. Transitions *down* \rightarrow *up* will be observed when the lifetime of the down state becomes comparable to or smaller than the experimental time, taken as the inverse rate of change of H_0 , while on the contrary, transitions *up* \rightarrow *down* will be

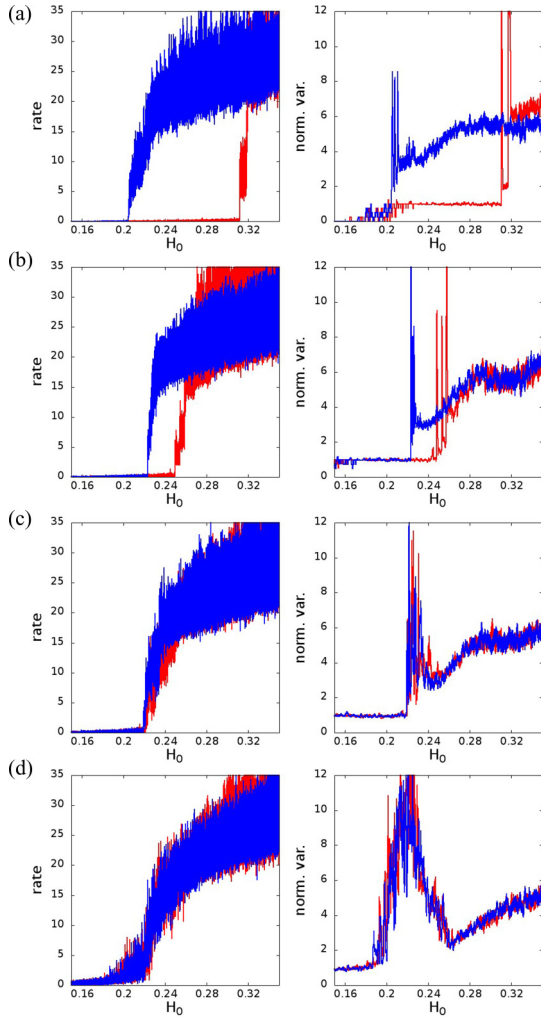


FIG. 2. Firing rate and normalized variance during spontaneous dynamics while sweeping H_0 at fixed α for $N = 3000$ and $P = 2$, and for values of the noise (a) $\alpha = 0.015$, (b) $\alpha = 0.03$, (c) $\alpha = 0.045$, and (d) $\alpha = 0.1$, showing a hysteretic behavior at low values of the noise. The strength of connections H_0 is increased from $H_0 = 0.1$ to $H_0 = 0.4$ during the first 50 s of the simulation (red line) and then decreases back to $H_0 = 0.1$ during the last 50 s (blue line), with a linear schedule. Transitions between two dynamical states, a “down” state with low rate and normalized variance equal to 1 and an “up state” with a much higher rate and normalized variance $F > 3$ are observed at different values of H_0 while ramping up or down, showing hysteresis at low values of the noise. Peaks in the normalized variance signal the transitions. At high values of the noise, $\alpha \geq 0.045$, there is an interval of H_0 , around $H_0 = 0.22 \approx 0.24$, where multiple transitions $down \rightarrow up$ and $up \rightarrow down$ are observed.

observed when the lifetime of the up state becomes smaller than the experimental time. At high values of the noise or at small system sizes, the lifetime of both up and down states becomes smaller than the experimental time, so that an alternation of up and down states can be observed.

In Fig. 4, the phase space of the system for $N = 3000$ (a) and $N = 12000$ (b) is shown. A red line marks the boundary where the dynamics switches from down to the up state when H_0 increases, at a fixed value of α , while a blue line marks the boundary from up state to down state when H_0 decreases.

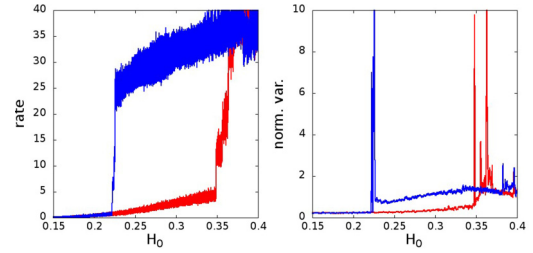


FIG. 3. Firing rate and normalized variance while sweeping H_0 as in Fig. 2 for $N = 12000$ and $P = 10$, and noise $\alpha = 0.01$. The hysteretic behavior is robust with respect to increasing size and number of patterns.

Bars indicate the width of the region where the transition may happen, namely, the lowest and highest values of H_0 where the transition was observed, for several realizations of the patterns and of the stochastic noise. Inside the strip defined by the bars, one may observe multiple back and forth transitions, i.e., an alternation of down and up states.

Red and blue lines can be interpreted as “pseudospinodal” lines that mark the point where the lifetime of the state (or nucleation time) becomes smaller than the observation time. While in systems with short range connections the nucleation time is independent from the size of the system, when connections are long range, as in our case, we expect that the nucleation times grow with the size of the system. Indeed, as shown in Fig. 4(b), by increasing the number of neurons from $N = 3000$ to $N = 12000$, the hysteresis region broadens, showing that lifetime of the states increases.

This means that the convergence of the “pseudospinodal” lines at $\alpha = 0.045$, for $N = 3000$, is actually a finite size effect, but the transition is still first order at these values of the parameters. As shown in the inset of Fig. 4(b), for $N = 12000$ lines meet at a much higher value of the noise, and a higher value of H_0 . It is reasonable to expect that, in the thermodynamic limit $N \rightarrow \infty$, the point where lines meet will tend to a definite value of α and H_0 , corresponding to a second-order transition point, terminating the first-order transition line.

To check the behavior of the nucleation time with network size, in Fig. 5 we investigate the nucleation time for network size $N = 12000, 7500, 3000$ at loading parameter $P/N = 1/1500$ and noise $\alpha = 0.03$. Notably, the nucleation time grows with the size of the system, supporting the hypothesis that metastable states have infinite lifetimes in the thermodynamic limit, as is expected for a system with long range interactions undergoing a first-order transition.

B. Critical behavior at the edge of instability

The presence of metastability and hysteresis indicates that the transition is a nonequilibrium first-order one. We here show that when one enters the metastable region from below, precursor phenomena in the form of scale-invariant spatiotemporal activity bursts can be observed that are distributed following power laws both in size and in duration.

Indeed, when approaching the $down \rightarrow up$ transition from below, before falling in the persistent up state, the network may have high fluctuations with transient periods of high activity.

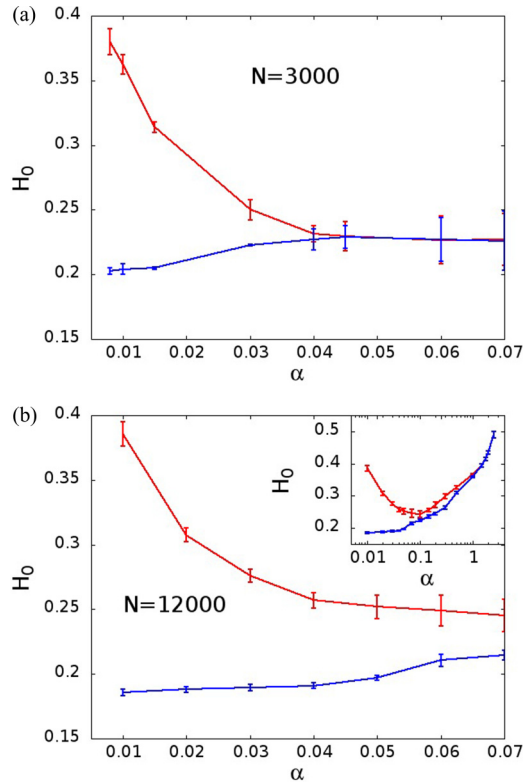


FIG. 4. (a) Hysteresis region and “pseudospinodal” lines for $N = 3000$ and $P = 2$. The red line marks the (average) value of H_0 where the dynamics switches from down to up state when H_0 increases, at a fixed value of α . The blue line the (average) value where the dynamics switches from up to down state when H_0 decreases. Bars indicate the lowest and highest values of H_0 where a transition was observed (with several different realizations of the stochastic noise). At high value of the noise, $\alpha > 0.04$, we observe no hysteresis, and bars indicate the interval in which multiple $down \rightarrow up$ and $up \rightarrow down$ transitions are observed. (b) Same plot for $N = 12000$ and $P = 2$. Lifetimes of the states increase with respect to the $N = 3000$ case, so that the up and down alternating region at these values of the noise disappears and the hysteresis region broadens. In the inset a larger range of parameters is investigated, showing that “pseudospinodal” lines merge at a higher value of noise and H_0 .

One can observe that inside this short period of high firing rate, at a finer level, the activity is made of a series of cascades or “avalanches,” separated by short drops in the rate, distributed with high diversity in spatiotemporal scale, resulting in power-law distributions.

We perform the following experiment: we fix a value of the noise α and connection strength H_0 , and simulate the spontaneous dynamics of the network. At low values of the noise, as the system is in a metastable state that has a finite lifetime, after some unpredictable time it will fall in the state of persistent replay of one of the stored patterns. We identify this event by looking when the average firing rate of the neurons stays above 10 Hz for an interval of time longer than 10 s. When the network falls in this “persistent up” state, we terminate the simulation and start the dynamics again from the beginning with a different realization of the noise. During the run before falling in the state of persistent replay, we measure the rate of

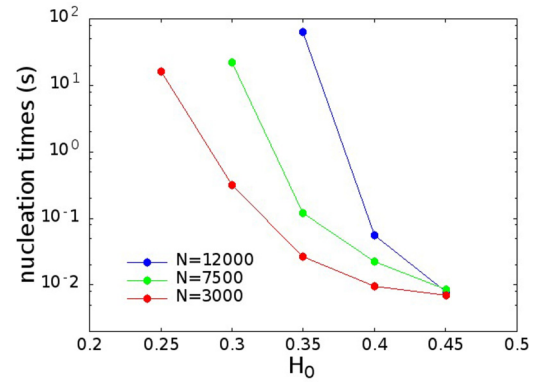


FIG. 5. Average nucleation times are shown for network sizes $N = 12000, 7500, 3000$ at a loading parameter $P/N = 1/1500$ and noise $\alpha = 0.03$, as a function of H_0 . Notably, the nucleation time grows with system size, as expected in a system with long range connections undergoing a first-order transition.

the network and identify the bursts of activity or avalanches. In Fig. 6(a), we show the rate during a run with $\alpha = 0.03$, $N = 3000$, and $H_0 = 0.22$. Note that in the last seconds of the simulation the rate remained above 10 Hz for 10 s, so the run was terminated. In the first 25 s, three bursts of activity can be seen, which were identified as a series of avalanches.

In contrast, for higher values of the noise, $\alpha \geq 0.045$ for $N = 3000$, the lifetime of the metastable states becomes smaller and one observes an interval of values of H_0 where the system shows bursts of activity, with short up and down alternation, without ever falling into the state of persistent replay, as shown in Fig. 6(b). Indeed, in this model with structured connectivity and replay of stored patterns, the noise has a twofold effect: on one hand it stimulates the start of a burst of activity, i.e., initiates a short collective replay of one of the stored patterns, but on the other hand, it can also stop its propagation and therefore hinder its persistent replay.

Note that up and down alternations, with bursts of generalized spiking that last for many seconds, have been observed to occur spontaneously in a variety of systems and conditions, both *in vitro* [40,41] and *in vivo* [42,43]. These bursts are composed by many avalanches.

As recently pointed out in Ref. [38], two different methods have been used to define avalanches. The first is based on the temporal proximity of neural activity, so that if activity happens in contiguous time bins, it is considered as belonging to the same avalanche. The second takes into account the causality of firing so that the activity of two neurons belong to the same avalanche if the spike of the first neuron directly causes the second neuron to fire. A novel tool for detect cascades of causally related events experimentally has been found, and it shows that indeed, neuronal avalanches are not merely composed of causally related events [44]. We define avalanches according to first method, that is, the one used in experiments, where causal information is not usually accessible. In particular, we use the methods implemented by Refs. [10,45,46], which altered the original method used by Ref. [1], to make it more suitable when the activity of a large number of neurons is measured. In Ref. [46], both methods were used, finding consistent results. Avalanches are

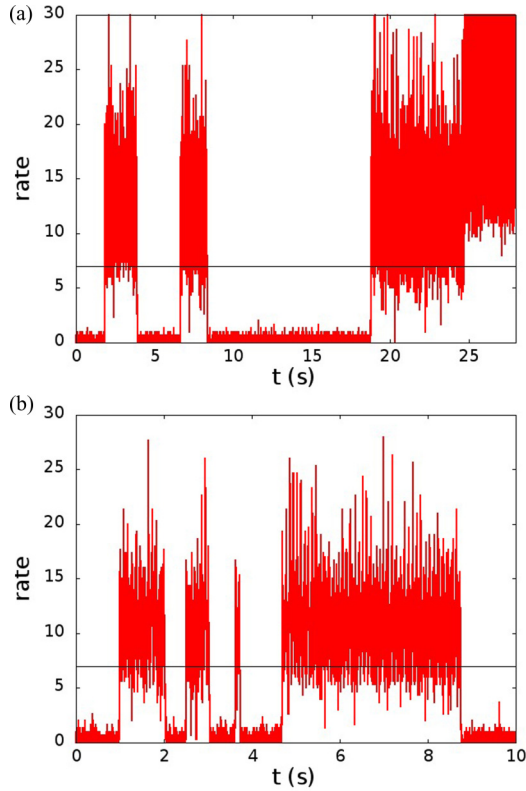


FIG. 6. Firing rate at fixed values of the noise and connection strength for (a) $\alpha = 0.03$, $H_0 = 0.22$ and (b) $\alpha = 0.045$, $H_0 = 0.22$, at $N = 3000$. At lower values of the noise, the system eventually falls into a state of “persistent up.” We identify this as an interval of 10 s where the rate is always larger than 10 Hz (last seconds of simulation in A) and stop the simulation. Avalanches are identified as consecutive time bins of $\Delta t = 1$ ms, with a rate higher than a threshold $R_{\min} = 7$ Hz. Three or four intervals [in (a) and (b), respectively] in which the system is in an up state are shown that are in turn composed of many avalanches.

therefore defined as periods of time where the population firing rate exceeds a threshold. As the population firing rate distribution is bimodal, reflecting the existence of the two phases, we set the threshold slightly higher than the minimum of the bimodal rate distribution, to minimize the probability of concatenating different avalanches. The minimum slightly changes with system size; therefore we use a threshold of $R_{\min} = 7$ Hz at $N = 3000$, and $R_{\min} = 10$ Hz at $N = 6000$ and 12 000, using a time bin of $\Delta t = 1$ ms to measure the population firing rate. Note that the rate is defined in terms of average spiking rate of single neurons; therefore a rate R in Hz corresponds to $RN/1000$ spikes per milliseconds, where N is the number of neurons. We define the size of an avalanche as the total number of spikes, that is, the integral of the rates over the avalanche duration.

In Figs. 7(a) and 7(b), we show the distribution of the sizes and durations of the avalanches for $\alpha = 0.06$ and $N = 3000$ near the pseudospinodal line, $H_0 = 0.22$, and both above and below it. We find a clear subcritical behavior at $H_0 = 0.19$, where the system mostly remains in the down state with very low activity, a scale-free behavior at $H_0 = 0.22$ where up-down alternation emerges, and a supercritical behavior with

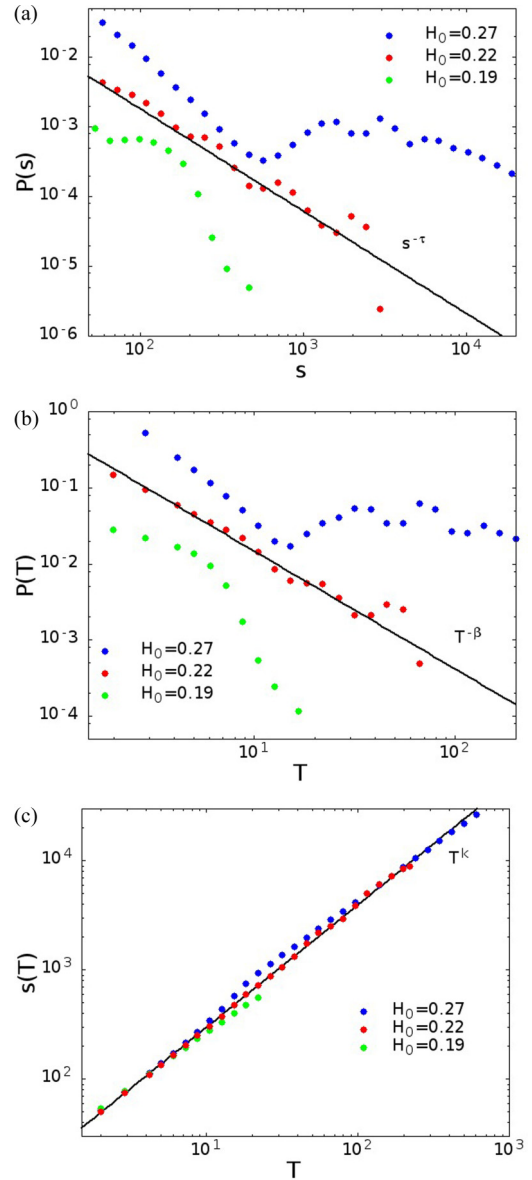


FIG. 7. (a) Size and (b) duration distribution of the avalanches at $N = 3000$, $P = 2$, and $\alpha = 0.06$ (curves are shifted for clarity). For $H_0 = 0.19$ a subcritical behavior is observed. Power laws are observed near the pseudospinodal at $H_0 = 22$, where the system shows alternation of up and down states. Increasing the value of H_0 above the pseudospinodal, the distribution shows a peak signaling a supercritical behavior. The exponents of power laws are $\tau = 1.47 \pm 0.1$ for the sizes, and $\beta = 1.55 \pm 0.1$ for the durations. (c) Average size of the avalanche as a function of the duration. The dependence is always a power law, with an exponent $k = 1.12 \pm 0.01$, in agreement with Eq. (3) within errors.

an excess of large avalanches above the pseudospinodal line at $H_0 = 0.27$. At $H_0 = 0.22$, near the pseudospinodal line, the distributions are well described by power laws, with an exponent $\tau = 1.47 \pm 0.1$ for the sizes and $\beta = 1.55 \pm 0.1$ for the durations.

We used the “powerlaw” PYTHON package [47] to compute the log-likelihood ratio of the power-law fit with respect to an exponential fit, finding $R = 76$ for the size and $R = 14$ for the

duration (positive values mean that power law is more likely), with a significance $p < 10^{-40}$ in both cases, indicating that the power-law fit is much better than the exponential fit.

While the exponent τ of the sizes is compatible with the largest part of the experimentally measured values, the value of β found originally (and predicted by models based on a branching process) was $\beta = 2$ [1]. However, values similar to the one found here have been observed in some experiments, for example, $\beta = 1.7 \pm 0.2$ in Ref. [25].

In Fig. 7(c), we show the average size of the avalanche as a function of its duration, that follows a power law with an exponent $k = 1.12 \pm 0.01$, which is in agreement, within errors, with the value predicted by the relation

$$k = \frac{\beta - 1}{\tau - 1}. \quad (3)$$

This relation was derived in Ref. [48] in relation to crackling noise.

It can also be derived by this simple reasoning: For values of the duration T' lower than the power-law cutoff T^* , the probability that an avalanche has a duration $T > T'$ goes as $P(T > T') \approx (T')^{1-\beta}$, and analogously, $P(s > s') \approx (s')^{1-\tau}$ if s' is lower than the cutoff s^* . Now if s' is the average size of an avalanche of duration T' , and fluctuations in the size fixed the duration and can be neglected, then $P(s > s') \approx P(T > T')$. It follows that $(T')^{k(1-\tau)} \approx (T')^{1-\beta}$ and therefore k satisfies Eq. (3), at least for sizes and durations below the cutoff. Notably, the relation $s(T) \approx T^k$ holds also quite far from critical regime, both experimentally [25] and in our model [see Fig. 7(c)].

Note that the branching process, which is usually connected with the critical behavior in cortical networks, predicts values of $\tau = 1.5$ and $\beta = 2$, so that $k = 2$, substantially greater than the one that we observe. On the other hand, different experiments reported values of the exponent lower than 2, and more similar to the value that we have measured [24,25], with τ and β satisfying the relation (3).

A value of k slightly larger than 1 is in agreement with the fact that avalanches are segments of collective spatiotemporal patterns, having a constant average rate of spikes, so that the total size of the avalanche is almost proportional to its duration, except for the beginning and end of the burst. The shape of avalanches in the branching process, on the other hand, corresponds to a rate of spikes having a maximum proportional to the duration T of the avalanche, giving rise to a total size proportional to T^2 .

It is interesting that relation (3) between the critical exponents is verified in our model and experimentally [24,25], while it is not verified in models where power law is not a manifestation of a critical point [49].

In Fig. 8, we show the avalanche distribution at $N = 3000$, 6000, 12 000, $P = 2$, $\alpha = 0.06$ and respectively for $H_0 = 0.22$, 0.23, and 0.265. The parameters for $N = 12 000$ are inside the hysteresis region of Fig. 4, where lifetime of the metastable state is longer than experimental time, and near the spinodal instability. The distributions follow power laws with exponents compatible within errors for different sizes, and with experimental results [6,25]. For $N = 12 000$ the exponents found are $\tau = 1.52 \pm 0.05$ for the sizes, and $\beta = 1.58 \pm 0.05$ for the durations. Also, in this case we compared the power-law

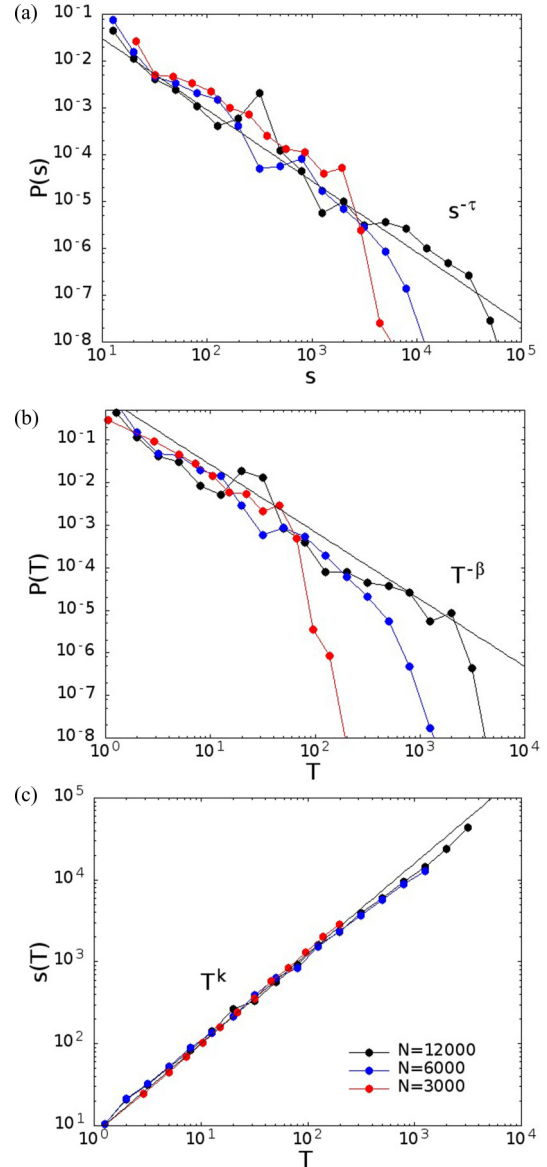


FIG. 8. (a) Size and (b) duration distribution of the avalanches at $N = 3000$, 6000, and 12 000, $P = 2$, $\alpha = 0.06$, and near the spinodal instability at $H_0 = 0.22$, 0.23, and 0.265, respectively. For $N = 12 000$ the exponents are $\tau = 1.52 \pm 0.05$ for the sizes and $\beta = 1.58 \pm 0.05$ for the durations. (c) Average size of the avalanche as a function of the duration for the same values of α and H_0 . For $N = 12 000$ the exponent of the power law is $k = 1.09 \pm 0.05$, in agreement with Eq. (3) within errors, taking points with duration $T < 50$. Note that for higher values of the duration the exponent seems to decrease and tend to 1, as observed in Ref. [25].

fits with the exponential ones, finding a log-likelihood ratio $R = 6.2$ for the sizes and $R = 7.2$ for the durations, with a significance $p < 10^{-10}$ in both cases. Notably, as reported in Figs. 8(a) and 8(b), the cutoff of the avalanche distributions scales with system size, supporting the scale-free behavior of the model near the pseudospinodal line. As shown in Fig. 8(c), the average size as a function of the duration follows a power law also at large sizes, with an exponent $k = 1.09 \pm 0.05$ at $N = 12 000$, which is again in agreement within errors with the

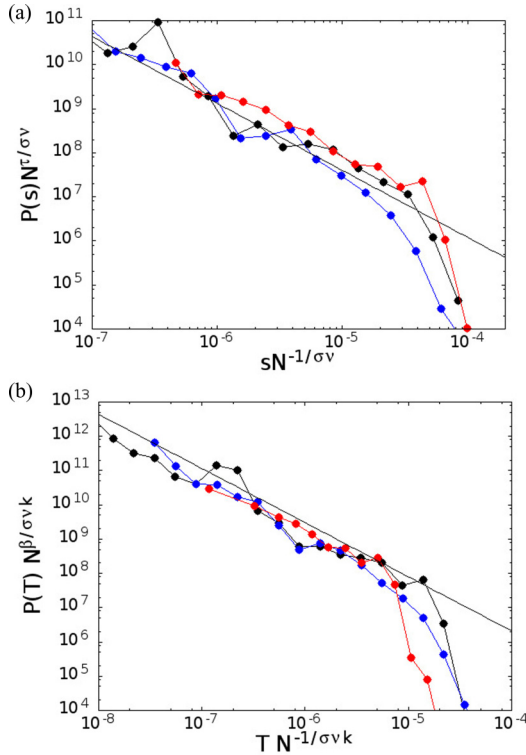


FIG. 9. Data collapse of the size (a) and duration (b) distributions of the avalanches. The exponent $1/\sigma\nu$ describes the dependence of the cutoff of the sizes as a function of the system size at the critical point $s_{\max} \propto N^{1/\sigma\nu}$, while for the durations $T_{\max} \propto N^{1/\sigma\nu k}$.

value predicted by relation (3) and with experimental results [24,25]. In Figs. 9(a) and 9(b), we show the finite size data collapse of the avalanche size and duration distribution. It is expected that the cutoff of the sizes and durations respectively scale as $s^* \propto N^{1/\sigma\nu}$ and $T^* \propto N^{1/\sigma\nu k}$ at the critical point, and their distributions are given by

$$P(s) = N^{-\frac{\tau}{\sigma\nu}} \tilde{P}_s(s/s^*),$$

$$P(t) = N^{-\frac{\beta}{\sigma\nu k}} \tilde{P}_T(T/T^*),$$

where $\tilde{P}_s(x)$ and $\tilde{P}_T(T)$ are master curves that go as $\tilde{P}_s(x) \propto x^{-\tau}$ and $\tilde{P}_T(x) \propto x^{-\beta}$ at small values of x . The best data collapse is given by a value $1/\sigma\nu = 2.2$ of the exponent.

Note that due to the heterogeneity and quenched disorder in the network connectivity, the region with scale-free avalanches of activity in the model is not limited to a single point or a single line in the phase space but is an extended region, similar to a Griffiths phase [50]. A broad region of hysteresis is observed, and at high noise or small size where there is no hysteresis a broad region of up-down alternation with burst composed of scale-free avalanches is observed.

III. DISCUSSION

Scale-free avalanches and critical behavior in cortical dynamics are frequently associated with second-order (continuous) phase transitions. However, power-law and critical phenomena also emerge in first-order phase transitions as one

enters the metastability region and approaches the spinodal line in systems with long range interactions [17,18].

A nonequilibrium first-order phase transition can be induced by additive noise [23,51] in spatially extended systems where coupling favors coherent behavior. By varying the parameters of the systems, or the noise, the order of the phase transition may change. A first-order phase transition with a coexistence region where the system displays hysteresis and a crossover to a second-order transition for large values of the noise has been studied in a variety of systems such as surface growth [52]. Hysteresis in a stochastic nonleaky integrate-and-fire model has been studied in [53], but scale-free avalanches were not investigated. A pioneer model that has hypothesized a new scenario for cortical dynamics, combining self-organized criticality with a first-order transition, is the one studied in Refs. [36,54,55]. More recently [56] it has been suggested that cortical networks are not self-organized to a critical point (SOC), as usually considered, but to a region of bistability (SOB) near a first-order transition. A most referenced model that displays criticality in a network of leaky integrate-and-fire neurons has been studied in Ref. [37]. In that model, however, criticality emerges only with a definition of avalanches that takes into account the causality of different firings. If one uses a criterion based only on temporal binning and proximity, as done usually in experiments where causality is not observable, one finds an exponential distributions of avalanches and no critical behavior is observed [38].

In this paper, we studied a model of leaky integrate-and-fire neurons, characterized by structured long range connectivity, corresponding to the encoding of spatiotemporal patterns. We showed that the model exhibits a first-order transition between a down state characterized by low activity and an up state characterized by the collective replay of one of the spatiotemporal patterns encoded in the network. Notably, the role of noise is crucial. Indeed, depending on the noise and size of the system, one observes hysteresis (low noise or large size) or up-down alternation (high noise or small size) at the transition.

Increasing the size of the system, the lifetimes of states increase, and one observes hysteresis also for values of the noise that showed alternation of states at smaller sizes, showing that the alternating behavior is a finite size effect and the underlying transition is of a first-order kind. Both in the region of hysteresis, approaching the spinodal instability, and in the region of alternation, we observe scale-free bursts of activity (avalanches). Notably, this was found by identifying avalanches using the same criterion of temporal proximity used in experiments.

While scale-free avalanches alone are not sufficient to assess criticality [49,57,58], we have independently identified a (first-order) transition by the discontinuity in the rate and the hysteretic behavior. Power-law distributions, and a peak in the normalized variance, are then observed near the edge of the spinodal instability, as is expected for a first-order transition in a model with long range connections.

The model therefore incorporates both criticality and the functioning of the network as a memory, or reservoir of dynamical patterns. When the system is posed at the edge of the instability, it shows spontaneous ongoing activity with critical scale-free behavior. However the state is a metastable one. If a

cue stimulation (a short train of input spikes, with order similar that of the stored patterns) is given, then the system switches in the persistent up state and responds with a (noncritical) sustained replay of the pattern stimulated. This behavior is similar to that observed experimentally in Ref. [24], where a transient state characterized by large noncritical avalanches is observed in response to an external stimulus.

The exponents of the size and duration distribution, and the exponent k giving the dependence of the size on the duration of the avalanche, $s(T) \approx T^k$, are compatible with the range of values found experimentally [6,24,25]. The value of k near to 1 is due to the mechanism of avalanche propagation. Indeed, in our case avalanches are segments of patterns having an almost constant average spiking rate so that the total size is almost proportional to the duration.

In a branching process model [59] it was shown that exponents of size and duration distributions are not universal but vary depending on a small external driving of the system. The effect of the driving, in the class of branching processes that they consider, is to merge smaller avalanches to form larger ones; therefore the relative weight of larger avalanches increases and exponents decrease with the driving, while the exponent k remains equal to 2 independent of the driving. In our model, on the other hand, avalanches are related to the emergence of a collective coordinated activity. Therefore the effect of noise is not only to merge avalanches, but also to hinder their propagation, decreasing the probability of longer avalanches. A higher noise decreases the lifetime of the metastable states, and hysteresis turns into up-down alternation, and even higher noise makes the region of up-down alternation broader.

Another paper that has considered the effect of the noise is Ref. [60]. They studied a “cortical branching model” that has a nonequilibrium phase transition only in the limit of zero spontaneous activation (that has a similar role of our noise), and a quasicritical behavior on the Widom line at finite values of the spontaneous activation, with a broadening of susceptibility. Also in our case we observe a broadening of the susceptibility (normalized variance) with the increase of the noise. However, in our model we observe a (first-order) transition also at nonzero values of the noise that produces (for not too low noise) an alternation between up and down states. Therefore the broadening of the variance is not connected to a Widom line but to the broadening of the region where alternation of up and down states is observed.

The main characteristic of our model is the structure of the connections, which are not chosen randomly but are the result of a learning rule inspired by spike-time-dependent plasticity (STDP), where different spatiotemporal patterns (corresponding to different sequences of firing of the neurons) are encoded. Connections are set at the beginning and held fixed during the dynamics of the network. Due to the fact that the learning kernel has a zero integral over time (see Appendix), connections are characterized by a balance between excitation and inhibition, which is one of the ingredients to observe a critical behavior, as observed experimentally [11,61] and also in models [62]. However, balance is not the only ingredient, since the topology and structure of the connectivity, with collective patterns carved as attractors of the dynamics, are crucial to observe the nonequilibrium first-order transition.

Preliminary results indeed indicate that by reshuffling the connections randomly between neurons, the transition disappears. One observes, on the contrary, a continuous increasing of the spiking rate when the strength of the connections is increased, with a normalized variance always near to 1, showing that the dynamics is Poissonian, and no critical behavior is observed [63]. This is also in agreement with recent results showing that topology is crucial for the emergence of critical states [64].

The presence of a nonequilibrium first-order transition and the critical precursor phenomena in our model are crucially related to the interplay between noise and a connectivity which promotes collectivity. Criticality emerges naturally near the edge of an instability, in an associative memory network, with many metastable dynamical states.

Another model that studies criticality together with associative memory was proposed in [65]. In their model, a Hebbian learning rule is used to store static patterns. However, they found that Hebbian learning alone destroys criticality even when the synaptic strength is properly scaled. Applying an optimization procedure that drives the synaptic couplings either toward the critical regime or toward the memory state in an alternating fashion, they finally arrive at a configuration both critical and that retains an associative memory. The reason why in our model the learning procedure does not destroy criticality may be due to the difference in the learning rule, that in our case is based on STDP and stores dynamical attractors as opposed to static ones.

Previous studies based on the branching process have explained the repeatability of spatiotemporal patterns [66,67] together with power laws in avalanche distribution. In their model, however, patterns are not shown to be attractors of the dynamics in any parameter space region. They show repeatability only in the critical region, where the dynamics is “neutral” (Lyapunov exponent equal to zero). On the other hand, in our model the stored spatiotemporal patterns emerge as collective attractors of the dynamics in the region above the transition. The systems is therefore both able to work as a stimulus-activated reservoir of spatiotemporal attractors and as a more flexible device when used at the border of the instability.

In our model, an alternation of up and down states is obtained with a fixed value of the excitability H_0 inside a certain range of external parameters near the transition. The same value of H_0 , lowering the noise, gives rise to hysteresis, with persistence of one or the other state depending on the previous history. However, it is plausible that the brain is able to change its state also by changing the value of H_0 , going out of the critical region toward a persistent up (more suited for either spontaneous or cue-triggered reactivation of previous experience) or down state (which favors faithful representation of sensory inputs) depending on the different behavioral state. For example Ref. [68] shows that focused attention pulls the system out of criticality towards subcriticality. The switch between different states, between sleep and wakefulness or from inattentive to vigilant states, may be induced by specific neuromodulators that, among other effects, can also change the efficacy of the connections. Neuromodulation is important for regulating brain states [69], but the specific mechanisms of these switchings are not yet well understood.

Another important ingredient of the network connectivity in our model is the presence of a small percentage of

neurons that have higher incoming connection strengths and are responsible for focusing the noise and initiating the collective activity (and avalanche propagation). The presence of a few highly active sites, driving cortical neural activity (leaders), has been reported experimentally [29,70–72]. Notably it has been shown that these leader sites are reliably and rapidly recruited within both spontaneous and evoked bursts [71]. As shown in Ref. [70], initiation of bursts of collective activity in cultured networks is a noise-driven nucleation phenomenon. The nucleation sites seem to be highly localized; they collect and amplify activity originated elsewhere. This noise focusing effect is realized in the present model with a higher H_0 to incoming connections to a bunch of neurons, which focus noise and cooperate to initiate the emergence of the pattern.

There are some predictions that could be investigated in experiments to discriminate between the first-order transition scenario considered here and other models. A prediction is that, lowering the noise, the lifetime of the states increases, and the system goes from a phase with alternation of up and down states to a phase characterized by metastability and hysteresis. The noise can be related, for example, to spontaneous neurotransmitter release. Another prediction of our model is that, increasing the strength of the connections but maintaining the balance between excitation and inhibition, the patterns that in the critical region appear during the alternation of up and down states become more attractive and can be replayed for a longer time. To our knowledge this kind of experiment has not been realized. What has been done is something quite different, that is, changing the balance between excitation and inhibition. This tunes the network into a phase characterized by high activity, far from the critical regime and with an excess of long avalanches. It is not clear, however, if this corresponds to the same kind of transition that we observe.

This work is a leaky integrate-and-fire model which shows how both dynamical attractors and neuronal avalanches converge in a single cortical model, and therefore may help to link the bridge between criticality and the need to have a reservoir of spatiotemporal metastable memories.

Note added in proof. Recently, we became aware that an argument similar to that following Eq. (3) was given in Ref. [73].

APPENDIX: THE MODEL

We simulate a network of N spiking neurons, modeled as leaky integrate-and-fire units and represented by the spike response model [74], in the presence of a Poissonian noise distribution. We study the spontaneous dynamics of the neurons connected by a sparse structured connectivity in absence of any external inputs. Between consecutive spikes, the membrane potential of neuron i is given by

$$u_i(t) = \sum_j \sum_{t_i < t_j < t} J_{ij} [e^{-(t-t_j)/\tau_m} - e^{-(t-t_j)/\tau_s}] + \sum_{t_i < \hat{t}_i < t} J(\hat{t}_i) [e^{-(t-\hat{t}_i)/\tau_m} - e^{-(t-\hat{t}_i)/\tau_s}], \quad (\text{A1})$$

where J_{ij} is the synaptic strength between presynaptic neuron j and postsynaptic neuron i , t_j are the spiking times of neuron j coming after the last spike t_i of neuron i , \hat{t}_i are random times

extracted from a Poissonian distribution with rate $\rho = 1 \text{ ms}^{-1}$, $J(\hat{t}_i)$ is a Gaussian variable extracted at time \hat{t}_i with zero mean and standard deviation $\sqrt{\frac{\alpha N}{3000\rho} \sum_j J_{ij}^2}$, τ_m is the characteristic time of membrane ($\tau_m = 10 \text{ ms}$), and τ_s is the characteristic time of synapse ($\tau_s = 5 \text{ ms}$). When the membrane potential $u_i(t)$ hits the threshold $\Theta = 1$, it is reset to zero and spikes are transmitted to all the neurons that receive input from neuron i . The strengths of the connections are determined by a learning rule [34,35,75,76], inspired by STDP (spike-time-dependent plasticity), which gives rise to a highly heterogeneous and disordered distribution of weights.

We build the connections J_{ij} forcing the network to store P spatiotemporal patterns. Each pattern is a periodic train of spikes, with one spike per neuron and per cycle, with the neuron i firing at times $t_i^\mu + nT$, with t_i^μ randomly and uniformly extracted in the interval $[0, T^\mu]$. In the present work, we use a number of neurons between $N = 3000$ and $N = 12000$, and a number of patterns between $P = 2$ and $P = 10$, with period $T^\mu = 333 \text{ ms}$. After the learning stage, the strength of connection J_{ij} is given by

$$J_{ij} = \frac{f_i H_0}{N} \sum_{\mu=1}^P \sum_{n=-\infty}^{\infty} A(t_i^\mu - t_j^\mu + nT^\mu), \quad (\text{A2})$$

where $A(\tau)$ is the STDP learning window [77,78] given by

$$A(\tau) = \begin{cases} a_p e^{-\tau/T_p} - a_D e^{-\eta\tau/T_p} & \text{if } \tau > 0, \\ a_p e^{\eta\tau/T_D} - a_D e^{\tau/T_D} & \text{if } \tau < 0, \end{cases} \quad (\text{A3})$$

with $a_p = A_0/[1 + \eta T_p/T_D]$, $a_D = A_0/[\eta + T_p/T_D]$, $A_0 = 3000$, $T_p = 10.2 \text{ ms}$, $T_D = 28.6 \text{ ms}$, and $\eta = 4$. To take account of the heterogeneity of the neurons, we use two values of f_i , $f_i = 1$ for “normal” neurons and $f_i = 3$ for “leader” neurons, i.e., neurons with higher incoming connection strengths, that amplify activity initiated by noise [29,70–72]. In other words, leaders are neurons that fire more than other ones and give rise to a cue able to initiate the short collective replay. They are chosen as a fraction of 3% of neurons with consecutive phases, for each pattern μ . The connection J_{ij} between neurons i and j does not depend therefore on the spatial distance between them if they are embedded in a two- or three-dimensional space. Therefore this form of the connections is a “long range” one, for which one could expect a “mean-field-like” behavior, with long lifetimes (infinite in the thermodynamic limit) of the metastable states. Long lifetimes can be expected also if connections are not independent from the distance, but the range is not too small.

Note that J_{ij} are proportional to N^{-1} , so that the noise is independent from N at fixed value of α . On the other hand, due to the shape of the STDP learning kernel that has a time integral equal to zero, this learning procedure assures the balance between excitation and inhibition, i.e., $\sum_j J_{ij}$ is of order $1/\sqrt{N}$. At the end of the learning procedure, part of the connections are positive (excitatory) and part are negative (inhibitory). Inhibitory neurons are not explicitly simulated, but negative connections can be considered as connections mediated by fast inhibitory interneurons. Alternatively, one could introduce a global inhibition and explicitly simulate only the positive connections.

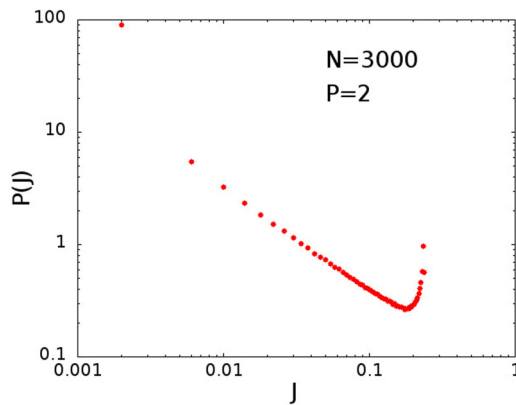


FIG. 10. Distribution of the positive connections after the learning procedure for $N = 3000$ neurons and $P = 2$ patterns.

The result of learning multiple spatiotemporal patterns, each with quenched randomly chosen phase ordering, gives rise to quenched disorder. The distribution of weight that results from this learning procedure is highly heterogeneous, with many small connections and a few strong ones. In Fig. 10

we show the distribution of the positive weights for $N = 3000$ neurons and $P = 2$ patterns. The distribution is very skewed and long-tailed, as observed in the cortex [79,80] and in other STDP-based models [81–83]. Note, however, that in our model the distribution of the weights is not a sufficient condition to determine the dynamical phase transition. Indeed, by shuffling the connections, leaving their distribution unchanged, this kind of transition disappears [63]. It seems therefore that the topology of the network, such as the relative abundance of motifs, is crucial for the manifestation of the first-order dynamical transition.

To get a sparse connectivity, like in the brain cortex, we prune the smallest connections. The pruning procedure still keeps the balance between excitation and inhibition and leaves only 30% of the original connections. Once this connectivity structure is built, it is kept fixed during all the network dynamics simulations.

Note that apart from the quenched random values of the times t_i^k defining the encoded patterns and f_i defining the leader neurons, the dynamics of the model depends only on the parameters α , determining the strength of the noise, and H_0 , determining the strength of the connections.

-
- [1] J. M. Beggs and D. Plenz, Neuronal avalanches in neocortical circuits, *J. Neurosci.* **23**, 11167 (2003).
 - [2] T. Petermann, T. C. Thiagarajan, M. A. Lebedev, M. A. L. Nicolelis, D. R. Chialvo, and D. Plenz, Spontaneous cortical activity in awake monkeys composed of neuronal avalanches, *PNAS* **106**, 15921 (2009).
 - [3] V. Pasquale, P. Massobrio, L. L. Bologna, M. Chiappalone, and S. Martinoia, Self-organization and neuronal avalanches in networks of dissociated cortical neurons, *Neuroscience* **153**, 1354 (2008).
 - [4] O. Shriki, J. Alstott, F. Carver, T. Holroyd, R. N. Henson, M. L. Smith, R. Coppola, E. Bullmore, and D. Plenz, Neuronal avalanches in the resting meg of the human brain, *J. Neurosci.* **33**, 7079 (2013).
 - [5] D. R. Chialvo, Emergent complex neural dynamics, *Nat. Phys.* **6**, 744 (2010).
 - [6] *Criticality in Neural Systems*, edited by D. Plenz and E. Niebur (Wiley, New York, 2014).
 - [7] P. Massobrio, L. de Arcangelis, V. Pasquale, H. Jensen, and D. Plenz, Criticality as a signature of healthy neural systems, *Front. Syst. Neurosci.* **9**, 22 (2015).
 - [8] V. Priesemann, M. Valderrama, M. Wibral, and M. Le Van Quyen, Neuronal avalanches differ from wakefulness to deep sleep — Evidence from intracranial depth recordings in humans, *PLoS Comput. Biol.* **9**, e1002985 (2013).
 - [9] O. Kinouchi and M. Copelli, Optimal dynamical range of excitable networks at criticality, *Nat. Phys.* **2**, 348 (2006).
 - [10] S. H. Gautam, T. T. Hoang, K. Mc Clanahan, S. K. Grady, and W. L. Shew, Maximizing sensory dynamic range by tuning the cortical state to criticality, *PLoS Comp. Bio.* **11**, e1004576 (2015).
 - [11] W. L. Shew, H. Yang, S. Yu, R. Roy, and D. Plenz, Information capacity and transmission are maximized in balanced cortical networks with neuronal avalanches, *J. Neurosci.* **31**, 55 (2011).
 - [12] H. Yang, W. L. Shew, R. Roy, and D. Plenz, Maximal variability of phase synchrony in cortical networks with neuronal avalanches, *J. Neurosci.* **32**, 1061 (2012).
 - [13] O. Shriki and D. Yellin, Optimal information representation and criticality in an adaptive sensory recurrent neuronal network, *Plos Comp. Biol.* **12**, e1004698 (2016).
 - [14] N. Tomen, D. Rotermund, and U. Ernst, Marginally subcritical dynamics explain enhanced stimulus discriminability under attention, *Front. Syst. Neurosci.* **8**, 151 (2014).
 - [15] D. Durstewitz, J. K. Seamans, and T. J. Sejnowski, Neurocomputational models of working memory, *Nat. Neurosci.* **3**, 1184 (2000).
 - [16] L. Minati, A. de Candia, and S. Scarpetta, Critical phenomena at a first-order phase transition in a lattice of glow lamps: Experimental findings and analogy to neural activity, *Chaos* **26**, 073103 (2016).
 - [17] D. W. Heermann, W. Klein, and D. Stauffer, Spinodals in a Long-Range Interaction System, *Phys. Rev. Lett.* **49**, 1682 (1982).
 - [18] D. W. Heermann, A. Coniglio, W. Klein, and D. Stauffer, Nucleation and metastability in three-dimensional Ising models, *J. Stat. Phys.* **36**, 447 (1984).
 - [19] S. Zapperi, P. Ray, H. E. Stanley, and A. Vespignani, Avalanches and damage clusters in fracture processes, *Lect. Notes Phys.* **567**, 452 (2001).
 - [20] S. Zapperi, P. Ray, H. E. Stanley, and A. Vespignani, First-Order Transition in the Breakdown of Disordered Media, *Phys. Rev. Lett.* **78**, 1408 (1997).
 - [21] J. B. Rundle, W. Klein, D. L. Turcotte, and B. D. Malamud, Precursory seismic activation and critical-point phenomena, *Pure Appl. Geophys.* **157**, 2165 (2000).
 - [22] A. Majdandzic, B. Podobnik, S. V. Buldyrev, D. Y. Kenett, S. Havlin, and H. E. Stanley, Spontaneous recovery in dynamical networks, *Nat. Phys.* **10**, 34 (2014).

- [23] A. A. Zaikin, J. García-Ojalvo, and L. Schimansky-Geier, Nonequilibrium first-order phase transition induced by additive noise, *Phys. Rev. E* **60**, R6275(R) (1999).
- [24] W. L. Shew, W. P. Clawson, J. Pobst, Y. Karimipناه, N. C. Wright, and R. Wessel, Adaptation to sensory input tunes visual cortex to criticality, *Nat. Phys.* **11**, 659 (2015).
- [25] N. Friedman, S. Ito, B. A. W. Brinkman, M. Shimono, R. E. Lee DeVille, K. A. Dahmen, J. M. Beggs, and T. C. Butler, Universal Critical Dynamics in High Resolution Neuronal Avalanche Data, *Phys. Rev. Lett.* **108**, 208102 (2012).
- [26] J. M. Beggs and D. Plenz, Neuronal avalanches are diverse and precise activity patterns that are stable for many hours in cortical slice cultures, *J. Neurosci.* **24**, 5216 (2004).
- [27] T. L. Ribeiro, S. Ribeiro, and M. Copelli, Repertoires of spike avalanches are modulated by behavior and novelty, *Front. Neural Circuits* **10**, 16 (2016).
- [28] D. Ji and M. A. Wilson, Coordinated memory replay in the visual cortex and hippocampus during sleep, *Nat. Neurosci.* **10**, 100 (2007).
- [29] A. Luczak and J. MacLean, Default activity patterns at the neocortical microcircuit level, *Front. Integr. Neurosci.* **6**, 30 (2012).
- [30] D. R. Euston, M. Tatsuno, and B. L. McNaughton, Fast-forward playback of recent memory sequences in prefrontal cortex during sleep, *Science* **318**, 1147 (2007).
- [31] K. Diba and G. Buzsáki, Forward and reverse hippocampal place-cell sequences during ripples, *Nat. Neurosci.* **10**, 1241 (2007).
- [32] M. A. Montemurro, M. J. Rasch, Y. Murayama, N. K. Logothetis, and S. Panzeri, Phase-of-firing coding of natural visual stimuli in primary visual cortex, *Curr. Biology* **18**, 375 (2008).
- [33] M. Siegel, M. R. Warden, and E. K. Miller, Phase-dependent neuronal coding of objects in short-term memory, *PNAS* **106**, 21341 (2009).
- [34] S. Scarpetta and A. de Candia, Neural avalanches at the critical point between replay and non-replay of spatio-temporal patterns, *PLoS One* **8**, e64162 (2013).
- [35] S. Scarpetta and A. de Candia, Alternation of up and down states at a dynamical phase-transition of a neural network with spatiotemporal attractors, *Front. Syst. Neurosci.* **8**, 88 (2014).
- [36] A. Levina, J. M. Herrmann, and T. Geisel, Phase Transitions Towards Criticality in a Neural System with Adaptive Interactions, *Phys. Rev. Lett.* **102**, 118110 (2009).
- [37] D. Millman, S. Mihalas, A. Kirkwood, and E. Niebur, Self-organized criticality occurs in non-conservative neuronal networks during up states, *Nat. Phys.* **6**, 801 (2010).
- [38] M. Martinello, J. Hidalgo, A. Maritan, S. di Santo, D. Plenz, and M. A. Muñoz, Neutral Theory and Scale-Free Neural Dynamics, *Phys. Rev. X* **7**, 041071 (2017).
- [39] F. Barbieri and N. Brunel, Can attractor network models account for the statistics of firing during persistent activity in prefrontal cortex? *Front. Neurosci.* **2**, 114 (2008).
- [40] R. Cossart, D. Aronov, and R. Yuste, Attractor dynamics of network up states in the neocortex, *Nature (London)* **423**, 283 (2003).
- [41] Y. Shu, A. Hasenstaub, and D. A. McCormick, Turning on and off recurrent balanced cortical activity, *Nature (London)* **423**, 288 (2003).
- [42] C. H. Petersen, T. G. Hahn, M. Mehta, A. Grinvald, and B. Sakmann, Interaction of sensory responses with spontaneous depolarization in layer 2/3 barrel cortex, *PNAS* **100**, 13638 (2003).
- [43] A. Luczak, P. Barthó, S. L. Marguet, G. Buzsáki, and K. D. Harris, Sequential structure of neocortical spontaneous activity in vivo, *PNAS* **104**, 347 (2007).
- [44] R. V. Williams-García, J. M. Beggs, and G. Ortiz, Unveiling causal activity of complex networks, *Europhys. Lett.* **119**, 1 (2017).
- [45] S. S. Poil, R. Hardstone, H. D. Mansvelder, and K. Linkenkaer-Hansen, Critical-state dynamics of avalanches and oscillations jointly emerge from balanced excitation/inhibition in neuronal networks, *J. Neurosci.* **32**, 9817 (2012).
- [46] T. Bellay, A. Klaus, S. Seshadri, and D. Plenz, Irregular spiking of pyramidal neurons organizes as scale-invariant neuronal avalanches in the awake state, *eLIFE* **4**, e07224 (2015).
- [47] J. Alstott, E. Bullmore, and D. Plenz, A Python package for analysis of heavy-tailed distributions, *Plos One* **9**, e95816 (2014).
- [48] J. P. Sethna, K. A. Dahmen, and C. R. Myers, Crackling noise, *Nature (London)* **410**, 242 (2001).
- [49] J. Touboul and A. Destexhe, Power-law statistics and universal scaling in the absence of criticality, *Phys. Rev. E* **95**, 012413 (2017).
- [50] P. Moretti and M. A. Muñoz, Griffiths phases and the stretching of criticality in brain networks, *Nat. Commun.* **4**, 2521 (2013).
- [51] R. Muller, K. Lippert, A. Kühnel, and U. Behn, First order nonequilibrium phase transition in a spatially extended system, *Phys. Rev. E* **56**, 2658 (1997).
- [52] L. Giada and M. Marsili, First-order phase transition in a nonequilibrium growth process, *Phys. Rev. E*, **62**, 6015 (2000).
- [53] A. Kaltenbrunner, V. Gómez, and V. López, Phase transition and hysteresis in an ensemble of stochastic spiking neurons, *Neural Comput.* **19**, 3011 (2007).
- [54] A. Levina, J. M. Herrmann, and T. Geisel, Dynamical synapses causing self-organized criticality in neural networks, *Nat. Phys.* **3**, 857 (2007).
- [55] A. Levina, J. M. Herrmann, and T. Geisel, Theoretical neuroscience of self-organized criticality: From formal approaches to realistic models, in *Criticality in Neural Systems*, edited by D. Plenz and E. Niebur (Wiley, New York, 2014).
- [56] S. di Santo, R. Burioni, A. Vezzani, and M. A. Muñoz, Self-Organized Bistability Associated with First-Order Phase Transitions, *Phys. Rev. Lett.* **116**, 240601 (2016).
- [57] J. Touboul and A. Destexhe, Can power-law scaling and neuronal avalanches arise from stochastic dynamics? *PLoS One* **5**, e8982 (2010).
- [58] J. M. Beggs and N. Timme, Being critical of criticality in the brain, *Front. Physiol.* **3**, 163 (2012).
- [59] S. di Santo, P. Villegas, R. Burioni, and M. A. Muñoz, Simple unified view of branching process statistics: Random walks in balanced logarithmic potentials, *Phys. Rev. E* **95**, 032115 (2017).
- [60] R. V. Williams-Garcia, M. Moore, J. M. Beggs, and Gerardo Ortiz, Quasicritical brain dynamics on a nonequilibrium Widom line, *Phys. Rev. E* **90**, 062714 (2014).
- [61] A. Mazzoni, F. D. Broccard, E. Garcia-Perez, P. Bonifazi, M. E. Ruaro, and V. Torre, On the dynamics of the spontaneous activity in neuronal networks, *Plos One* **2**, e439 (2007).
- [62] F. Lombardi, H. J. Herrmann, and L. de Arcangelis, Balance of excitation and inhibition determines 1/f power spectrum in neuronal networks, *Chaos* **27**, 047402 (2017).

- [63] I. Apicella, S. Scarpetta, and A. de Candia, *Structured Versus Shuffled Connectivity in Cortical Dynamics* (Springer, New York, 2016), p. 323.
- [64] P. Massobrio, V. Pasquale, and S. Martinoia, Self-organized criticality in cortical assemblies occurs in concurrent scale-free and small-world networks, *Sci. Rep.* **5**, 10578 (2015).
- [65] M. Uhlig, A. Levina, T. Geisel, and J. M. Herrmann, Critical dynamics in associative memory networks, *Front. Comput. Neurosci.* **7**, 87 (2013).
- [66] C. Haldeman and J. M. Beggs, Critical Branching Captures Activity in Living Neural Networks and Maximizes the Number of Metastable States, *Phys. Rev. Lett.* **94**, 058101 (2005).
- [67] W. Chen, J. P. Hobbs, A. Tang, and J. M. Beggs, A few strong connections: Optimizing information retention in neuronal avalanches, *BMC Neurosci.* **11**, 3 (2010).
- [68] E. D. Fagerholm, R. Lorenz, G. Scott, M. Dinov, P. J. Hellyer, N. Mirzaei, C. Leeson, D. W. Carmichael, D. J. Sharp, W. L. Shew, and R. Leech, Cascades and cognitive state: Focused attention incurs subcritical dynamics, *J. Neurosci.* **35**, 4626 (2015).
- [69] S. H. Lee and Y. Dan, Neuromodulation of brain states, *Neuron* **76**, 209 (2012).
- [70] J. G. Orlandi, J. Soriano, E. Alvarez-Lacalle, S. Teller, and J. Casademunt, Noise focusing and the emergence of coherent activity in neuronal cultures, *Nat. Phys.* **9**, 582 (2013).
- [71] V. Pasquale, S. Martinoia, and M. Chiappalone, Stimulation triggers endogenous activity patterns in cultured cortical networks, *Sci. Rep.* **7**, 9080 (2017).
- [72] J-P. Eckmann, S. Jacobi, S. Marom, E. Moses, and C. Zbinden, Leader neurons in population bursts of 2d living neural networks, *New J. Phys.* **10**, 015011 (2008).
- [73] J. P. Coleman, K. A. Dahmen, and R. L. Weaver, Avalanches and scaling collapse in the large- N Kuramoto model, *Phys. Rev. E* **97**, 042219 (2018).
- [74] W. Gerstner and W. Kistler, *Spiking Neuron Models: Single Neurons, Populations, Plasticity* (Cambridge University Press, Cambridge, England, 2002).
- [75] S. Scarpetta, F. Giacco, and A. de Candia, Storage capacity of phase-coded patterns in sparse neural networks, *Europhys. Lett.* **95**, 28006 (2011).
- [76] S. Scarpetta and F. Giacco, Associative memory of phase-coded spatiotemporal patterns in leaky integrate and fire networks, *J. Comp. Neurosci.* **34**, 319 (2013).
- [77] G. Q. Bi and M. M. Poo, Precise spike timing determines the direction and extent of synaptic modifications in cultured hippocampal neurons, *J. Neurosci.* **18**, 10464 (1998).
- [78] H. Markram, J. Lubke, M. Frotscher, and B. Sakmann, Regulation of synaptic efficacy by coincidence of postsynaptic APs and EPSPs, *Science* **275**, 213 (1997).
- [79] S. Song, P. J. Sjöström, M. Reigl, S. Nelson, and D. B. Chklovskii, Highly nonrandom features of synaptic connectivity in local cortical circuits, *Plos Biol.* **3**, e350 (2005).
- [80] Y. Loewenstein, A. Kuras, and S. Rumpel, Multiplicative dynamics underlie the emergence of the log-normal distribution of spine sizes in the neocortex in vivo, *J. Neurosci.* **31**, 9481 (2011).
- [81] L. Yassin, B. L. Benedetti, J. S. Jouhanneau, J. A. Wen, J. F. Poulet, and A. L. Barth, An embedded subnetwork of highly active neurons in the neocortex, *Neuron* **68**, 1043 (2010).
- [82] F. Effenberger, J. Jost, and A. Levina, Self-organization in balanced state networks by STDP and homeostatic plasticity, *PLOS Comput. Biol.* **11**, e1004420 (2015).
- [83] Z. Tosi and J. Beggs, Cortical circuits from scratch: A metaplastic architecture for the emergence of lognormal firing rates and realistic topology, [arXiv:1706.00133](https://arxiv.org/abs/1706.00133).